

# Macromolecules

Volume 36, Number 5

March 11, 2003

© Copyright 2003 by the American Chemical Society

## Communications to the Editor

### Formation of Amphiphilic Polyion Complex Vesicles from Mixtures of Oppositely Charged Block Ionomers

Stefan Schrage, Reinhard Sigel, and  
Helmut Schlaad\*

Max-Planck-Institut für Kolloid- und  
Grenzflächenforschung, Abteilung Kolloidchemie,  
Am Mühlenberg 1, 14476 Golm, Germany

Received July 12, 2002

Revised Manuscript Received December 2, 2002

Block copolymers are widely used to generate nanostructured materials and to stabilize colloidal particles. One of the main features of block copolymers is their ability to form well-defined structures in solution and in the solid state.<sup>1</sup> In a selective solvent, spherical or cylindrical micelles or vesicles (polymersomes) are usually formed depending vastly on the concentration and the chemical composition of the copolymer. However, the phase behavior is drastically changed when additional energy contributions from electrostatic or other interactions come into play. Ionomers (i.e., copolymers with an ionic content of less than ~15 mol %)<sup>2</sup> and interpolyelectrolyte complexes, for instance, exhibit a very broad range of micellar and vesicular morphologies and other hierarchical superstructures.<sup>3</sup>

Inspired by the work of Harada and Kataoka on polyion complex (PIC) micelles,<sup>4</sup> we started to investigate pairs of oppositely charged ionomers having different solvating blocks. By choosing strongly segregating polymers,<sup>1</sup> we were hoping to generate polyion complex micelles with a corona composed of two microphase-separated polymer segments, so-called "Janus micelles"<sup>5</sup> (named after the two-faced Roman god Janus), or other superstructures with a reduced symmetry. Basically, we could imagine two different kinds of superstructures,

namely (i) clusters of Janus micelles<sup>5</sup> and (ii) vesicles having a microphase-separated membrane. For a stoichiometric PIC of poly(1,2-butadiene)<sub>216</sub>-*block*-poly(cesium methacrylate)<sub>29</sub>, **1**, and polystyrene<sub>211</sub>-*block*-poly(1-methyl-4-vinylpyridinium iodide)<sub>33</sub>, **2**, in tetrahydrofuran (THF), we believe to have found the second structure: vesicles with a polybutadiene (PB) inside and a polystyrene (PS) outside, as illustrated in Figure 1. These vesicles are amphiphilic in nature even though they have a centrosymmetric structure! A somewhat related but inverse structure of vesicles with preferentially segregated acidic and basic corona chains has only recently been reported—to our best knowledge for the first time—by Luo and Eisenberg.<sup>6</sup>

The block ionomer samples **1** and **2** were prepared by anionic polymerization and subsequent modification reactions as reported elsewhere.<sup>1a</sup> Briefly, 1,3-butadiene was polymerized at -78 °C in THF with *sec*-butyllithium as the initiator in the presence of LiCl. The living polybutadienyllithium was end-capped with 1,1-diphenylethylene, and then *tert*-butyl methacrylate was added as the second monomer. After the polymerization was complete and quenched with degassed methanol, the polymer was precipitated in aqueous ethanol, filtered, and dried in a vacuum at +35 °C to constant weight. According to NMR and standard size exclusion chromatography (SEC), the synthesized polybutadiene-*block*-poly(*tert*-butyl methacrylate) copolymer has 216 butadiene (93% 1,2 and 7% *trans*-1,4) and 29 methacrylic units; the apparent polydispersity index (PDI) is 1.07. This precursor polymer was transformed into **1** by a HCl-catalyzed hydrolysis of ester groups and subsequent neutralization with CsOH. The quantitative modification of methacrylate units was confirmed by NMR and FT-IR analysis.

By the same polymerization procedure, a polystyrene-*block*-poly(4-vinylpyridine) sample with 211 styrene and 33 4-vinylpyridine units (NMR and SEC) and a PDI of ~1.2 (SEC) was synthesized. The quaternization of the pyridine moieties with methyl iodide afforded **2** in virtually quantitative yield (NMR).

\* To whom correspondence should be addressed: phone ++49-331-567-9514; Fax ++49-331-567-9502; e-mail schlaad@mpikg-golm.mpg.de.

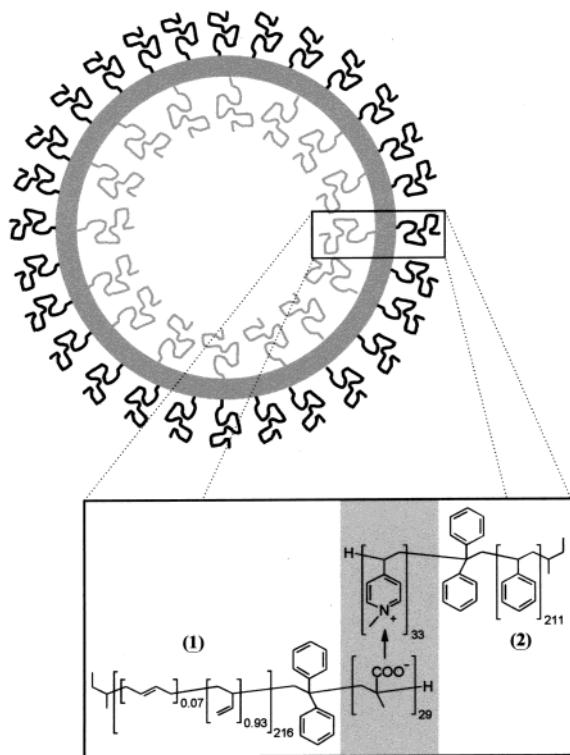


**Figure 1.** Schematic model of a vesicle with a corona of segregated polymer chains, as formed in a mixture of oppositely charged block ionomers.

We first examined the dilute solutions of these two block ionomers by dynamic and static light scattering (DLS/SLS).<sup>7</sup> It is known that the analysis of the aggregation behavior of ionomers with LS is complicated and often produces difficult to evaluate data.<sup>8</sup> The dimension of aggregates and aggregation numbers (= average number of ionomer chains per aggregate,  $Z$ ) obtained from DLS and SLS measurements are therefore considered as rough estimates. Also, the values of the ratio  $R_g/R_h$  ( $R_g$  = radius of gyration,  $R_h$  = hydrodynamic radius) are losing significance in the determination of the structure of aggregates.

For 0.003–0.25 wt % solutions of **1** and **2** in THF ( $T = 25^\circ\text{C}$ ), DLS showed the presence of large aggregates with  $R_h \sim 75$  and  $50$  nm, respectively. Note that THF is a nonsolvent for the charged block segments; therefore, the solvating or stabilizing corona of these aggregates should be composed of either PB ( $\rightarrow$ **1**) or PS ( $\rightarrow$ **2**). Sample **1**, which is rather poorly soluble in THF ( $<0.8$  mg/mL), seemed to form stable aggregates only when the concentration was below  $0.02$  wt %. At higher concentrations, the size of aggregates was steeply increasing ( $R_h > 120$  nm), which might be attributed to coagulation or the formation of some kind of clusters. In the case of **2**, on the other hand, the size of aggregates remained the same in the whole concentration range investigated. It should further be noted that there was no evidence for a dissociation of aggregates or of a polyelectrolyte effect. For these two samples, SLS provides  $R_g$  values in the same order as  $R_h$  and aggregation numbers of  $\sim 1000$  and  $700$ , respectively.

Upon mixing the solutions of oppositely charged block ionomers **1** and **2** ( $[-]/[+] = 1.0$ ), we expect that a neutral PIC **3** will be formed, accompanied by the release of CsI (which to a certain extent is soluble in THF). First DLS measurements indicated that in  $0.01$ –

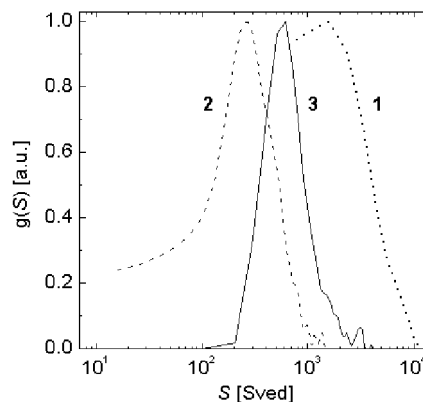


**Figure 2.** Sedimentation coefficient distributions  $g(S)$  obtained for the  $0.1$  wt % solutions of the block ionomers **1** and **2** and the PIC **3** in THF at  $25^\circ\text{C}$ .

$0.25$  wt % solutions of **3** in THF aggregates with  $R_h = 65$ – $80$  nm are present. Although the CONTIN analysis of the DLS data provided monomodal size distributions, diffusion coefficients showed a nonlinear dependence on the scattering vector. This indicates that the sample exhibits a considerable polydispersity. Like for the previous samples, similar values for  $R_h$  and  $R_g$  were obtained. The aggregation number was estimated to be  $\sim 1200$ —somewhat higher than for the aggregates of the pure block ionomers. It appears that, because of this very high  $Z$  value and from simple geometric considerations ( $R_h > l_c$ , contour length of polymer chains), we can exclude a micellar structure of the aggregates.<sup>9</sup> The only aggregates that could exhibit such large dimensions are clusters of micelles or hollow vesicular aggregates.

The samples were further characterized with analytical ultracentrifugation (AUC);<sup>10</sup> sedimentation–velocity runs were applied to fractionate  $0.1$  wt % THF solutions of **1**–**3**. The sedimentation coefficient distributions (see Figure 2) of **1** and **2** were broad with a peak value of the sedimentation coefficient ( $S$ ) of  $\sim 1590$  and  $270$  Sved, respectively. The distribution, which was obtained for the mixed sample **3**, was considerably narrower and exhibited a maximum at  $S \sim 600$ . These and LS results confirm that the mixing of the oppositely charged block ionomers produced a novel PIC species, which again was forming stable aggregates in dilute THF solution. Obviously, the steric stabilization by the hydrophobic corona chains could not prevent the ionomer aggregates from coalescence followed by polyion complexation.

From  $S$  and  $R_h$  values we calculated an average density of the aggregates of the PIC **3** of  $0.922$  g  $\text{cm}^{-3}$ .<sup>11</sup> This value ranges between the density of THF ( $0.889$  g  $\text{cm}^{-3}$ ) and the bulk densities of PB ( $0.96$  g  $\text{cm}^{-3}$ ) and PS ( $1.04$  g  $\text{cm}^{-3}$ ).<sup>12</sup> To our opinion, this low density of PIC aggregates points to a hollow vesicular structure rather than a compact cluster. It further suggests that the released CsI, which has a density as high as  $4.51$  g  $\text{cm}^{-3}$ , was partly if not completely extracted from the polymer and transferred into the THF phase, thus fixing the structure of aggregates.

To determine the structure of aggregates formed by the PIC **3**, we applied transmission electron microscopy (TEM).<sup>13</sup> The micrograph in Figure 3A shows spherical aggregates which are about  $100$ – $200$  nm in diameter. (Note, the specimen was prepared by drying a  $0.01$  wt % THF solution of **3** on a carbon-coated grid.) This is in reasonable agreement with the results obtained from LS indicating that the original dimension of aggregates

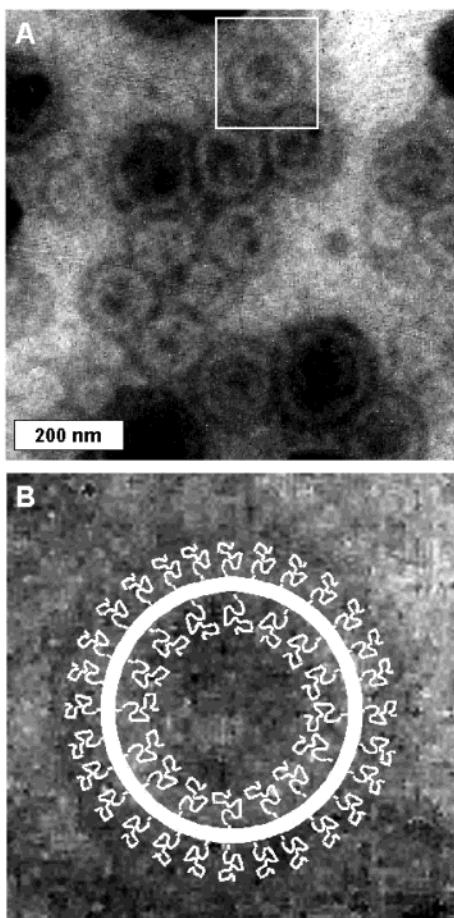


**Figure 3.** (A) TEM micrograph of the vesicular aggregates of the PIC **3** (negatively stained with CsI), prepared from a 0.01 wt % THF solution. (B) Magnification of the framed area in (A), showing an individual vesicular aggregate.

had been well preserved during the preparation of the TEM specimen. However, these aggregates could only be visualized by TEM because the original solution contained small amounts of CsI (see above), which acts as a negative staining agent. All attempts to stain the PB segments by exposing the specimen to OsO<sub>4</sub> vapor were not successful. The dark rings, which can be observed in the TEM micrograph, originate from CsI being accumulated at the outer surface of the aggregates upon evaporation of the solvent. The dark spots inside the aggregates indicate that these are hollow spheres, which were originally filled with solvent containing some CsI. These results, besides the ones obtained from LS and AUC, support a vesicular structure of the PIC aggregates. The thickness of the collapsed polymer membrane, which in TEM shows as a bright layer between the dark regions (cf. Figure 3B), was estimated to be ~30 nm.

Figure 4 shows the TEM picture of a microtomed and selectively stained (OsO<sub>4</sub>) polymer film, prepared by slowly evaporating a 0.1 wt % vesicular THF solution of **3**. One can see a rather regular pattern of spherical PB domains (dark) embedded in a PS matrix (bright) and nothing like a lamellar or hexagonal morphology which one might have expected regarding the volume fractions of the two hydrophobic segments ( $\Phi_{PB}/\Phi_{PS} \sim 0.6$ ).<sup>1</sup> We can only explain the occurrence of such a "cubic" morphology if we assume that the PIC vesicles originally had a phase-separated microstructure, as shown in Figure 1, and maintained their structure

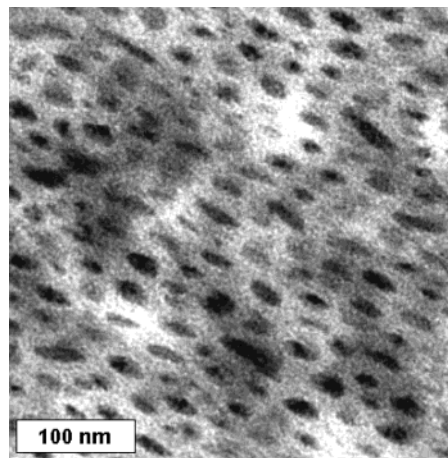


**Figure 4.** TEM micrograph of a microtomed and OsO<sub>4</sub>-stained polymer film, prepared from a 0.1 wt % THF solution of the PIC **3**.

during the preparation of the specimen. Basically, this separation of phases within the membrane originates from the strong incompatibility of the two hydrophobic segments ( $\chi N \sim 40$ ;  $\chi$  = Flory–Huggins interaction parameter and  $N$  = degree of polymerization). It is reasonable that PS rather than PB forms the external layer because of its higher space requirements ( $\Phi_{PS} > \Phi_{PB}$ ). This microphase-separated structure of the PIC vesicle membrane might be the explanation why the attempts to stain the PB segments for the above-described TEM analysis failed, the PS outer layer shielding the PB from the OsO<sub>4</sub> vapor.

There are some very interesting features connected with this kind of superstructure, which in the future shall be pursued in detail. First, these vesicles are amphiphilic in nature and should therefore adopt a different morphology when exposed to a solvent with another quality or selectivity. For instance, the addition of a selective solvent like hexane to a solution of PIC vesicles in THF might cause an inversion of the original structure; i.e., PB instead of PS then would be at the outer surface of the membrane. For PIC vesicles prepared in a  $\Theta$  solvent for one of the hydrophobic segments, e.g., cyclohexane, it might also be possible to induce a reversible "switching" between these two morphologies by changing the temperature.<sup>3</sup> Second, polyion complexation is a reversible process;<sup>3</sup> thus, the PIC vesicles might disintegrate upon the addition of a low-molecular-weight acid or base—first experiments with malonic acid seem to confirm this hypothesis. Presumably, the carboxylic acid replaces the anionic component of the PIC vesicle, which is then repelled from the membrane.

Finally, and this is the most important aspect of this work, we obtained a novel complex morphology via a modular approach, just by mixing two different diblock copolymers with a most simple primary structure. Here, we made use of electrostatic interactions to control the formation of the superstructure, but other specific interactions like hydrogen bonding or donor–acceptor interactions could also be applied. Such a modular concept allows to produce a library of complex superstructures with adjustable properties for special applications. Water-soluble amphiphilic PIC vesicles, made from biocompatible block ionomers, could for instance be used as advanced drug carrier systems.



**Acknowledgment.** We thank Prof. Markus Antonietti, Ines Below, Dr. Helmut Cölfen, Dr. Jürgen Hartmann, Magdalena Losik, Rona Pitschke, Marc Schneider, Antje Völkel, and Erich C. for their contributions to this work. This work is financially supported by the Max-Planck-Gesellschaft.

## References and Notes

- (1) See for example: (a) Förster, S.; Antonietti, M. *Adv. Mater.* **1998**, *10*, 195. (b) Discher, B. M.; Hammer, D. A.; Bates, F. S.; Discher, D. E. *Curr. Opin. Colloid Interface Sci.* **2000**, *5*, 125. (c) Bates, F. S.; Fredrickson, G. H. *Phys. Today* **1999**, *52*, 32. (d) Bates, F. S.; Fredrickson, G. H. *Annu. Rev. Phys. Chem.* **1990**, *41*, 525.
- (2) Eisenberg, A.; Kim, J.-S. *Introduction to Ionomers*, John Wiley & Sons: New York, 1998.
- (3) See for example: (a) Zhang, L. F.; Eisenberg, A. *Science* **1995**, *268*, 1728. (b) Gohy, J.-F.; Varshney, S. K.; Jérôme, R. *Macromolecules* **2001**, *34*, 2745. (c) Kirkmeyer, B. P.; Taubert, A.; Kim, J.-S.; Winey, K. I. *Macromolecules* **2002**, *35*, 2648. (d) Cornelissen, J. J. L. M.; Fischer, M.; Sommerdijk, N. A. J. M.; Nolte, R. J. M. *Science* **1998**, *280*, 1427. (e) Kukula, H.; Schlaad, H.; Antonietti, M.; Förster, S. *J. Am. Chem. Soc.* **2002**, *124*, 1658. (f) Harada, A.; Kataoka, K. *Macromolecules* **1995**, *28*, 5294. (g) Lysenko, E. A.; Bronich, T. K.; Eisenberg, A.; Kabanov, V. A.; Kabanov, A. V. *Macromolecules* **1998**, *31*, 4511. (h) Talingting, M. R.; Munk, P.; Webber, S. E.; Tuzar, Z. *Macromolecules* **1999**, *32*, 1593.
- (4) Harada, A.; Kataoka, K. *Science* **1999**, *283*, 65.
- (5) Erhardt, R.; Böker, A.; Zettl, H.; Kaya, H.; Pyckhout-Hintzen, W.; Krausch, G.; Abetz, V.; Müller, A. H. E. *Macromolecules* **2001**, *34*, 1069.
- (6) (a) Luo, L.; Eisenberg, A. *J. Am. Chem. Soc.* **2001**, *123*, 1012. (b) Luo, L.; Eisenberg, A. *Angew. Chem.* **2002**, *114*, 1043; *Angew. Chem., Int. Ed.* **2002**, *41*, 1001.
- (7) LS measurements were carried out at 25 °C with an ALV goniometer and an ALV-5000 digital correlator (ALV GmbH, Langen, Germany) with a frequency-doubled Neodym-YAG laser (Coherent DPSS532, intensity 300 mW,  $\lambda = 532$  nm) as the light source. DLS autocorrelation functions were measured at different concentrations and scattering angles and evaluated with the CONTIN method (Provencher, S. W. *Comput. Phys. Commun.* **1982**, *27*, 229). From the obtained diffusion coefficients ( $D$ ), hydrodynamic radii ( $R_h$ ) were calculated using the Stokes–Einstein equation. Apparent molecular weights of aggregates ( $M_{w,app}$ ), radii of gyration ( $R_g$ ), and second virial coefficients ( $A_2$ ) were determined by SLS from a Zimm plot. Refractive index increments ( $dn/dc$ ) were measured with a NFT-Scanref differential refractometer operating at  $\lambda = 633$  nm. However, these measurements provided uncommonly high  $dn/dc$  values for **1–3** ( $dn/dc = 0.3511$ ,  $0.4718$ , and  $0.3981$  cm<sup>3</sup> g<sup>-1</sup>, respectively); therefore, the values being reported in the literature (Brandrup, J., Immergut, E. H., Eds.; *Polymer Handbook*; John Wiley & Sons: New York, 1986; VII/409) for PB and PS in THF at 25 °C ( $\lambda = 546$  nm) were used to evaluate SLS data:  $dn/dc = 0.132$  (**1** ← PB),  $0.193$  (**2** ← PS), and  $0.172$  cm<sup>3</sup> g<sup>-1</sup> (**3** ← PB/PS, 35/65 w/w).
- (8) Schmidt, M., private communication.
- (9) Förster, S.; Zisenis, M.; Wenz, E.; Antonietti, M. *J. Chem. Phys.* **1996**, *104*, 9956.
- (10) AUC measurements were carried out with an Optima XL-I ultracentrifuge (Beckman-Coulter, Palo Alto, CA) equipped with Rayleigh interference and UV/vis absorption optics. Sedimentation velocity runs of 0.1 wt % solutions in THF were performed with 5000 rpm at 25 °C. Raw data were transformed into sedimentation coefficient distributions ( $g(S)$ ) using the SEDFIT software: Schuck, P. *Biophys. J.* **2000**, *78*, 1606.
- (11) Cölfen, H.; Pauck, T. *Colloid Polym. Sci.* **1997**, *275*, 175.
- (12) Brandrup, J., Immergut, E. H., Eds.; *Polymer Handbook*, 3rd ed.; John Wiley & Sons: New York, 1989; V/1 + V/82.
- (13) TEM studies were performed with a Zeiss EM 912 Omega operating at 120 kV. Specimens were prepared by placing a drop of 0.01 wt % solutions onto a 400 mesh carbon-coated copper grid; the solvent was left to evaporate at room temperature. Polymer films were obtained by solvent-casting and were ultramicrotomed at -20 °C with a Leica Ultracut UCT. Specimens with a thickness of 30–50 nm were transferred onto carbon-coated copper grids and were exposed to OsO<sub>4</sub> vapor for 3–5 min.

MA0255940